

## Photosensitive $n$ -In<sub>2</sub>O<sub>3</sub> / $p$ -InSe Heterojunctions with Nanostructured Surface of the Frontal Layer

Z.D. Kovalyuk<sup>1</sup>, V.M. Katerynychuk<sup>1</sup>, Z.R. Kudrynskyi<sup>1,\*</sup>, O.S. Lytvyn<sup>2</sup>

<sup>1</sup> *Frantsevich Institute for Problems of Materials Science of National Academy of Sciences of Ukraine, Chernivtsi Department, 5, Iryny Vilde Str., 58001 Chernivtsi, Ukraine*

<sup>2</sup> *Lashkaryov Institute of Semiconductor Physics of National Academy of Sciences of Ukraine, 41, Nauki Pr., 03028 Kyiv, Ukraine*

(Received 12 February 2013; published online 17 October 2013)

We report on photosensitive  $n$ -In<sub>2</sub>O<sub>3</sub> /  $p$ -InSe heterojunctions with nanostructured In<sub>2</sub>O<sub>3</sub> frontal layer. It was established that photoresponse spectra of the heterojunctions significantly depend on the surface topology of the oxide. This means that the oxide with semiconductor substrate is not only an active component of the structure, but also serves as a cell diffraction material. Surface topology of the oxide was studied by means of the atomic force microscope. At various conditions of oxidation of InSe the surface of the samples contained nanoformations preferably in the form of nanoneedles. Their location has both disordered and ordered character. A dimensional optical effect in the oxide was revealed due to the anisotropic light absorption in InSe. The higher deviation of incident light from its normal direction due to a nanostructured surface is, the higher variation in the generation of carriers in the semiconductor is. These changes consist in the energy broadening of the heterojunction photoresponse spectrum as well as in the peculiarities of the excitonic line. The higher density and ordering of the nanoneedles on the oxide surface is, the higher long-wave shift and more intensive excitonic peak in the spectrum takes place.

**Keywords:** Heterojunctions, Layered crystals, Nanostructures, Atomic force microscopy, Oxide films.

PACS numbers: 68.55. – a, 71.20.Be, 82.80.Pv, 81.16.Pr

### 1. INTRODUCTION

Phenomena of light diffraction and interference are usually observed using diffraction grating or diffraction grid. They have a periodic structure of transparent and opaque grooves or cells, whose sizes are comparable with the light wavelength. A question about the interaction of light and nanostructured surface, for which sizes of nanostructured objects are one order less than, for example, the width of grooves in diffraction gratings, is of a great interest. Nanostructured surface objects can have different topology and ordering depending on the production technique. Therefore, nanostructured surfaces should have different properties of light scattering.

Fabrication of heterostructures is one of the production methods of the surface with nanostructured relief. Growth of the frontal layer of heterostructure is usually accompanied by the formation of surface nanostructured objects [1]. Varying the growth conditions of this layer, one can influence the structure of surface elements.

Deviation of light from its initial direction will occur at normal light incidence on transparent nanostructured surface due to the dimensional optical effects. If use anisotropic crystals as a semiconductor substrate, then diffraction properties of the nanostructured surface will influence the photoelectric properties of heterojunctions produced on the basis of these anisotropic crystals.

InSe [2] and GaSe [3-5] layered crystals can be the examples of semiconductor substrates with strongly anisotropic properties. They are successfully used as the base of many heterojunctions due to the possibility of the production of qualitative substrates by means of cleavage [6-12]. In<sub>2</sub>O<sub>3</sub>-InSe structure is one of such hetero

structures. Photoresponse spectra of In<sub>2</sub>O<sub>3</sub>-InSe heterostructures with different localization of the  $p$ - $n$ -junction with respect to  $c$  differ for  $E_{\perp c}$  and  $E_{\parallel c}$  orientations of illumination, where  $E$  is the electric field vector of electromagnetic wave;  $c$  is the crystallographic axis [13]. At light propagation through nanostructured surface of the frontal layer conditions of the relative position of  $E$  and  $c$  vectors can be strongly changed. Therefore, the use of In<sub>2</sub>O<sub>3</sub>-InSe heterostructures, in which oxide surface is nanostructured and substrate is anisotropic one, serves as a perfect model for the discovery of the dimensional optical effects.

Nanosopic studies of the surface topology confirm the formation of nano-objects in freshly cleaved InSe crystals [14], in samples inclined to the action of probe of the atomic-force microscope [14, 15], and in proper oxides of these crystals [16, 17].

### 2. EXPERIMENTAL TECHNIQUE

InSe<Cd> crystals were used for the investigations. They were grown by the Bridgman method from non-stoichiometric composition of components of InSe compound and had  $p$ -type conduction [18]. Substrates of the crystals were cut from an ingot and represented plane-parallel plates with sizes of  $10 \times 5 \times 0.3$  mm<sup>3</sup>. Crystal samples were placed into electrical furnace for a while in air at temperature of 420 °C. Choice of the oxidation temperature is realized randomly. Samples were studied after oxidation in order to establish the surface topology of the oxide. To this end, atomic force microscope (AFM) Nanoscope IIIa Dimension 3000 SPM (Digital Instruments, USA) was used.

\* kudrynskyi@gmail.com

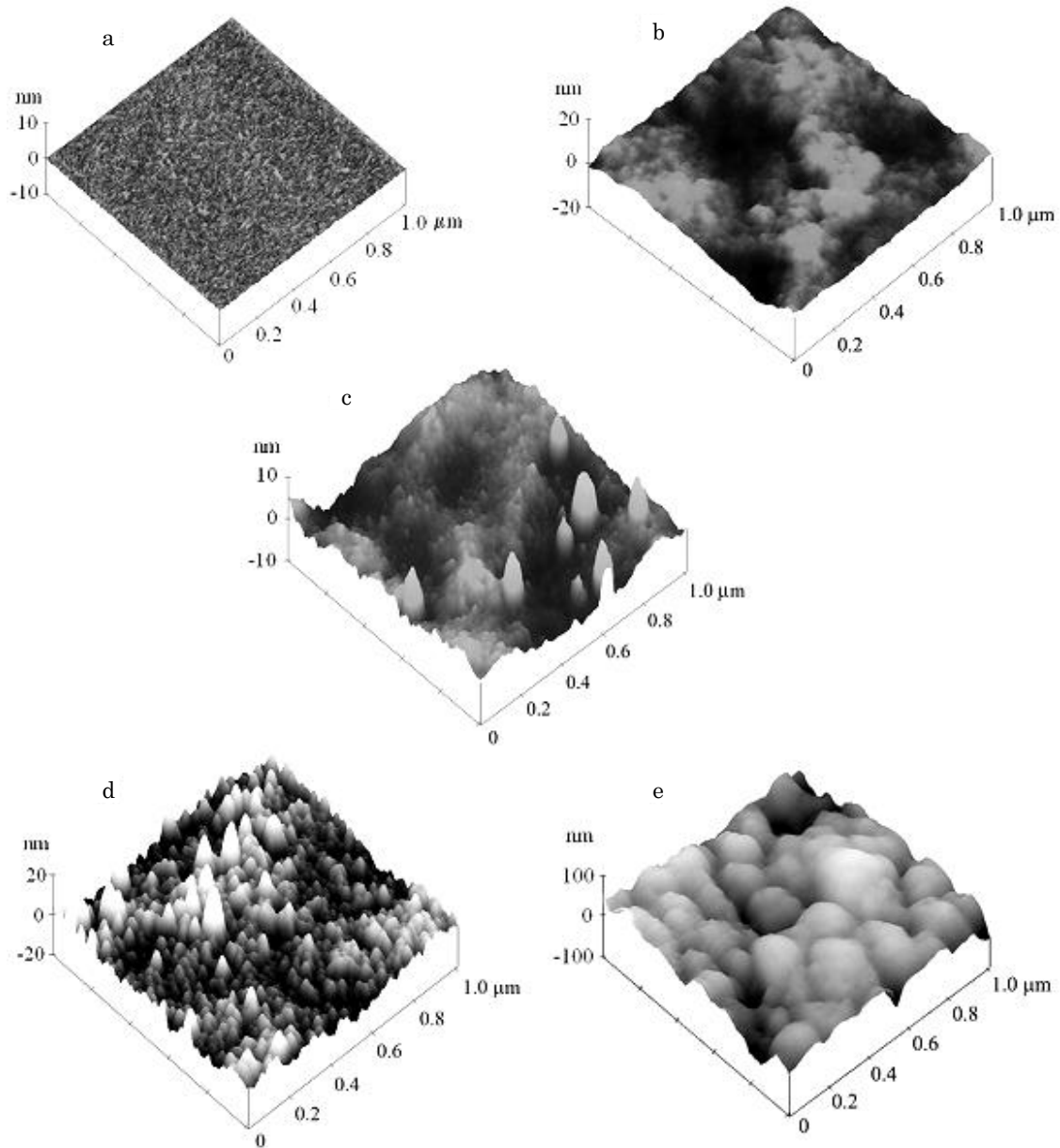


**Fig. 1** – Images of non-oxidized (a) and oxidized (b-e) InSe (0001) surface obtained using the atomic-force microscope: oxidation temperature and time are equal to 420 °C and 0.25 (b), 1 (c), 5 (d), and 20 hours (e), respectively

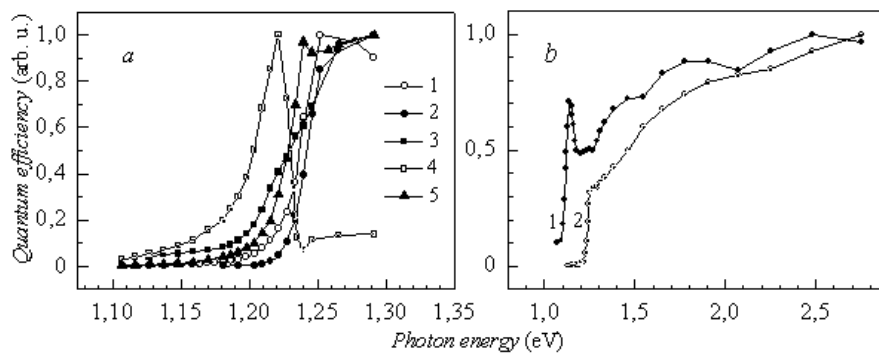


**Fig. 2** – Photoreponse spectra of the  $n\text{-In}_2\text{O}_3/p\text{-InSe}$  heterojunctions at room temperature. Geometry of illumination of the  $p\text{-}n$ -junction: a –  $E_{1c}$ ; 1 – 0; 2 – 0.25; 3 – 1; 4 – 5; and 5 – 20 hours of sample oxidation; b : 1 –  $E_{gc}$  and 2 –  $E_{1c}$

Due to the conductive properties of the oxide, oxidized samples represented a finished  $n$ - $\text{In}_2\text{O}_3$  /  $p$ - $\text{InSe}$  heterojunction sensitive to light [19]. However, to eliminate a current shorting, excess oxidized sides of the substrates were cut or cleaved except of one of two opposite planes which are the cleavage surfaces. Pure indium was used as contacts. Photoresponse spectra of heterostructures were studied by using the monochromator MDR-3 with resolution not worse than 13 Å/mm and normalized to 1.

### 3. EXPERIMENTAL RESULTS AND DISCUSSION

AFM images of the non-oxidized and oxidized  $\text{InSe}$  surface are represented in Fig. 1.

They imply that surface topology and sizes of oxide nano-objects can be varied by the operating modes of substrate oxidation. Consider some peculiarities of the surface topology. For non-oxidized  $\text{InSe}$  surface in the (0001) plane the arithmetical mean of its roughness  $R_a$  was equal to  $\sim 0.053$  nm (Fig. 1a). This value confirms the conclusion about high quality of the layered crystal cleavage. Clusters of oxide crystallites colored in white in Fig. 1b are formed on the  $\text{InSe}$  surface after sample oxidation during 15 minutes. They are formations of undefined shape and different density. Lateral crystallite sizes are about 100 nm. Height of separate crystallites determined by the cross-section method did not exceed 1 nm. For  $\text{InSe}$  samples oxidized during 1 hour (Fig. 1c), sizes of non-oxidized regions (dark color) decrease. The value of  $R_a$  increases up to  $\sim 0.631$  nm.

Separate crystallites take the form of nanoneedles, whose height reaches 10 nm. Appearance of such groups of nanoneedles can be connected with different time of their initiation on the  $\text{InSe}$  surface and features of the crystallite coalescence behavior. At the increase in the oxidation time up to 5 hours, a rather uniform ensemble of  $\text{In}_2\text{O}_3$  crystallites in the form of nanoneedles, which covers a whole surface of layered crystal, is formed on the  $\text{InSe}$  surface (Fig. 1d). As follows from the statistical analysis of the AFM image, surface density of nanoneedles is equal to  $\sim 4 \times 10^9$  cm $^{-2}$ . Average values of the sizes of nanoneedles in this case were equal in height  $h = 5.2 \pm 2.44$  nm and base  $d = 50.6 \pm 7.2$  nm. After sample oxidation during 20 hours oxide crystallites are transformed from the needle-like to the dome-like form (Fig. 1e). Height and base of oxide eminence reach 50 and 200 nm, respectively. So, by the optimization of the operating modes, which depend on the oxidation temperature and time, as well as heating and cooling modes of  $\text{InSe}$  layered crystal, an ordered ensemble of nanoneedles on the surface of  $\text{In}_2\text{O}_3$  oxide can be formed.

Photoresponse spectra of the  $n$ - $\text{In}_2\text{O}_3$  /  $p$ - $\text{InSe}$  heterojunctions are shown in Fig. 2, where spectra depending on the scheme of sample illumination are illustrated on the inset a and spectra in only one polarization  $E_{\perp c}$  but with different oxide topology – on the inset b.

Spectra in Fig. 2a show that their long-wave edge differs by the presence of an intensive peak ( $E_{\parallel c}$ ) and its absence at  $E_{\perp c}$  that is conditioned by  $\text{InSe}$  anisotropic

properties. This peak is ascribed to the formation of excitons. Absence of the peak in the  $E_{\perp c}$  polarization of illumination is connected with the fact that binding energy of excitons at this temperature is less than the thermal energy  $kT$  [20]. Shift of the long-wave spectral edge for different polarizations is conditioned by the difference in type (allowed or forbidden) of the interband transitions [21]. The same behavior of the spectra is also observed in the case of  $E_{\perp c}$ , but with different topology of nanostructured surface (Fig. 2b). The larger density of nanoneedles and the higher degree of their ordering on the oxide surface is, the more evident energy shift and more intensive exciton peak in the spectrum is (curve 4, Fig. 2b). For the case of the surface shown in Fig. 1d, shift of the photoresponse edge is maximum and equal to  $\sim 0.13$  eV. Decrease in the degree of ordering of the surface nano-objects (Fig. 1e) leads to both the decrease in the intensity of spectral exciton lines and decrease in its long-wave shift.

It follows from the aforesaid that there is a direct dependence between the structure of oxide surface and shape of the photoresponse spectra of  $n$ - $\text{In}_2\text{O}_3$  /  $p$ - $\text{InSe}$  heterojunctions. Here, ordered nanostructured objects play the role of diffraction grid with nanodimensional cells. Deviation of beams from the normal incidence is so strong that it corresponds to almost the case of the sample illumination in the  $E_{\parallel c}$  polarization. Since light absorption coefficient in  $\text{InSe}$  crystal is anisotropic and differs by the value about two orders of magnitude, then nanostructured surface can influence the region of photo-carrier generation in semiconductor. This influence can be exhibited in the change of the acquisition coefficient of photocarriers by a barrier toward its increase and can promote the optimization of photoelectric parameters of the studied heterojunction.

### 4. CONCLUSIONS

Conducting films of  $\text{In}_2\text{O}_3$  oxide are obtained by the oxidation in air of  $\text{InSe}$  crystals at the temperature of 420 °C. Different oxidation time influences the surface structure of the oxide which was studied using the AFM images. Oxide surface is nanostructured, and its objects change their topology depending on the duration of the oxidation process. The highest degree of ordering of the surface elements, representing an ensemble of nanoneedles, is obtained during 5 hour oxidation of  $\text{InSe}$ .

Influence of the nanostructured surface on the photoresponse spectra of  $n$ - $\text{In}_2\text{O}_3$  /  $p$ - $\text{InSe}$  heterojunctions, whose substrate is anisotropic, is investigated. Changes in the spectra are connected with the long-wave shift of the photoresponse edge and the formation of the edge exciton peak. These changes depend on the degree of ordering of the oxide surface elements, and the more appreciable they are, the higher ordering of nano-objects is. The same changes in the spectra take place at illumination of anisotropic  $\text{InSe}$  crystals in the  $E_{\perp c}$  and  $E_{\parallel c}$  polarizations. Comparison of the obtained results indicates the strong diffraction properties of nanostructured surface of the studied oxide.

## REFERENCES

1. N.N. Ledentsov, V.M. Ustinov, V.A. Shchukin, P.S. Kop'ev, Zh.I. Alferov, D. Bimberg, *Semiconductors* **32**, 343 (1998).
2. V.M. Katerynchuk, Z.R. Kudrynskyi, Z.D. Kovalyuk, *J. Nano-Electron. Phys.* **4**, 02042 (2012).
3. A.P. Bakhtinov, Z.R. Kudrynskyi, O.S. Litvin, *Phys. Solid State* **53**, 2154 (2011).
4. V.N. Katerinchuk, Z.D. Kovalyuk, V.V. Netyaga, T.V. Betsa, *Inorg. Mater.* **37**, 336 (2001).
5. L. Leontie, I. Evtodiev, V. Nedeff, M. Stamate, M. Caraman, *Appl. Phys. Lett.* **94**, 071903 (2009).
6. V.N. Katerinchuk, M.Z. Kovalyuk, *Tech. Phys. Lett.* **25**, 54 (1999).
7. V.N. Katerinchuk, Z.D. Kovalyuk, T.V. Betsa, V.M. Kaminskii, V.V. Netyaga, *Tech. Phys. Lett.* **27**, 424 (2001).
8. S.I. Drapak, V.B. Orletskii, Z.D. Kovalyuk, *Semiconductors* **38**, 546 (2004).
9. Z.D. Kovalyuk, V.P. Makhniy, O.I. Yanchuk, *Semicond. Phys. Quantum Electron. Optoelectron.* **6**, 458 (2003).
10. M.Z. Kovalyuk, V.I. Vitkovskaya, M.V. Tovarnitskii, *Tech. Phys. Lett.* **23**, 385 (1997).
11. R. Adelung, F. Ernst, A. Scott, M. Tabib-Azar, L. Kipp, M. Skibowski, S. Hollensteiner, E. Spiecker, W. Jäger, et al., *Adv. Mater.* **14**, 1056 (2002).
12. R.N. Bekimbetov, Yu.A. Nikolaev, V.Yu. Rud', Yu.V. Rud', E.I. Terukov, *Semiconductors* **34**, 1064 (2000).
13. Z.D. Kovalyuk, V.N. Katerinchuk, T.V. Betsa, *Opt. Mater.* **17**, 279 (2001).
14. K. Uosaki, M. Koinuma, *J. Appl. Phys.* **74**, 1675 (1993).
15. A.I. Dmitriev, V.V. Vishnyak, G.V. Lashkarev, V.L. Karbovskii, Z.D. Kovalyuk, A.P. Bakhtinov, *Phys. Solid State* **53**, 622 (2011).
16. Z.D. Kovalyuk, V.M. Katerynchuk, A.I. Savchuk, O.S. Lytvyn, *Superlattice. Microst.* **44**, 416 (2008).
17. V.M. Katerynchuk, Z.D. Kovalyuk, *Inorg. Mater.* **47**, 749 (2011).
18. A. Segura, J.P. Guesdon, J.M. Besson, A. Chevy, *J. Phys. Appl.* **14**, 253 (1979).
19. V.M. Katerynchuk, M.Z. Kovalyuk, *Pis'ma Zh. Tekh. Fiz.* **18**, 70 (1992).
20. J. Camassel, P. Merle, H. Mathieu, A. Chevy, *Phys. Rev. B.* **17**, 4718 (1978).
21. V.L. Bakumenko, Z.D. Kovalyuk, L.N. Kurbatov, V.F. Chishko, *Fiz. Techn. Poluprovodn.* **10**, 1045 (1976).